Effects of Moving Core Velocity and Viscous Dissipation on Fully Developed Laminar Heat Transfer in Concentric Annuli

by
Ganbat DAVAA*, Toru SHIGECHI**
and Satoru MOMOKI**

Fully developed laminar heat transfer of a Newtonian fluid in a concentric annulus with an axially moving core was analyzed taking into account the viscous dissipation of the flowing fluid. The effects of the relative velocity of a moving core and viscous dissipation on the temperature distributions and Nusselt numbers at the tube walls have been discussed.

1. Introduction

Problems involving fluid flow and heat transfer with an axially moving core of solid body or fluid in an annular geometry can be found in many manufacturing processes, such as extrusion, drawing and hot rolling, etc. In such processes, a hot cylindrical rod continuously exchanges heat with the surrounding environment. For such cases, the fluid involved may be Newtonian or non-Newtonian and the flow situations encountered can be either laminar or turbulent.

Another example which involves viscous dissipation effect is seen in microchannel cooling using liquid coolant[1]. The increasing scales of circuit integration of electronic components accompanied by reducing feature size of integrated circuit (IC) chips have increased the problems associated with cooling. Laminar regime viscous dissipation problems are widely involved in microchannel heat transfer such as efficient cooling techniques for IC chips.

In the previous report[2], exact solutions of the momentum and energy equations were obtained for fully developed laminar flow of Newtonian fluid flowing for an annular geometry. There the effects of viscous dissipation on heat transfer was omitted.

In this study the energy equation with the viscous dissipation term was exactly solved for the boundary conditions of constant wall heat flux at one tube wall with the other insulated.

Nusselt numbers at the inner and outer tubes were presented for the wide ranges of parameters: the radius ratio, the relative core velocity and Brinkman number.

Nomenclature

a_1, a_2	coefficients, Eq.(30), Eq.(31)
b_1, b_2	coefficients, Eq.(44), Eq.(45)
Br	Brinkman number, Eq.(15)
$c_1 \sim c_4$	coefficients, Eq.(26) ~Eq.(29)
c_P	specific heat at constant pressure
$d_1 \sim d_4$	coefficients, Eq.(40) ~Eq.(43)
k	thermal conductivity
Nu	Nusselt number
P	pressure
Pe	Peclet number $\equiv Re \cdot Pr$
Pr	Prandtl number
q	wall heat flux
r	radial coordinate
r^*	dimensionless radial coordinate $\equiv r / R_o$
R	radius
Re	Reynolds number $\equiv u_m \cdot 2 (R_o - R_i) / \nu$
T	temperature
u	fluid velocity
u^*	dimensionless fluid velocity $\equiv u / u_m$
u_m	average velocity
U	core velocity
U^*	relative core velocity $\equiv U / u_m$
z	axial coordinate
α	radius ratio $\equiv R_i / R_o$
η	dimensionless axial coordinate $\equiv z / \{2 (R_o - R_i) Pe\}$
θ	dimensionless temperature
μ	viscosity
ν	kinematic viscosity $\equiv \mu / \rho$
ρ	density
B	$\equiv (\alpha^2 - 1) / \ln \alpha$
B^*	$\equiv wB$
E	$\equiv \{\alpha^2 - (B/2)\} / (\alpha^2 - 1)$
M	$\equiv 1 + \alpha^2 - B$

Received on October 27, 2000

* Graduate School of Science and Technology
** Department of Mechanical Systems Engineering

w $\equiv \{1-(U^*/2)\}/(1-EU^*)$

subscripts

b	bulk
i	inner tube
ii	inner tube (Case A)
o	outer tube
oo	outer tube (Case B)

2. Analysis

The physical model for the analysis is shown in Fig.1. The outer tube is stationary and the core tube is axially moving at a constant velocity. The assumptions used in the analysis are:

1. The flow is incompressible and steady-laminar, and fully developed, hydrodynamically and thermally.
2. The fluid is Newtonian and physical properties are constant.
3. The body forces and axial heat conduction are neglected.

2.1 Fluid Flow

The momentum equation together with the assumptions described above is

$$\frac{1}{r}\frac{d}{dr}\left(r\frac{du}{dr}\right)=\frac{1}{\mu}\frac{dP}{dz} \tag{1}$$

The boundary conditions are:

$$\begin{cases} u = U & \text{at } r = R_i \\ u = 0 & \text{at } r = R_o \end{cases} \tag{2}$$

Solving Eq.(1) with Eq.(2), u is obtained as

$$u=\frac{2u_m}{M}(1-EU^*)\left(1-r^{*2}+B^*\ln r^*\right) \tag{3}$$

where u_m is the average velocity, given as

$$u_m \equiv \frac{1}{\pi(R_o^2-R_i^2)}\int_{R_i}^{R_o} u\cdot 2\pi r dr$$

$$= \frac{R_o^2}{4\mu}\left(-\frac{dP}{dz}\right)\frac{M}{2}+EU. \tag{4}$$

The dimensionless fluid velocity, u^*, is written as

$$u^*=\frac{2}{M}(1-EU^*)\left(1-r^{*2}+B^*\ln r^*\right) \tag{5}$$

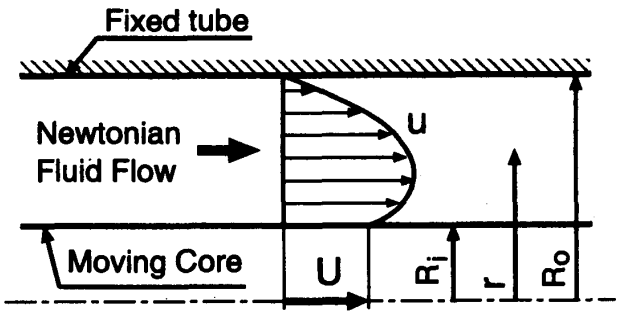

Fig.1 Schematic of a concentric annulus

$$\left(\frac{du^*}{dr^*}\right)^2=4\left(\frac{1-EU^*}{M}\right)^2\left[4r^{*2}-4B^*+\left(\frac{B^*}{r^*}\right)^2\right] \tag{6}$$

2.2 Heat Transfer

The energy equation together with the assumptions and constant wall heat flux condition is written as

$$k\frac{1}{r}\frac{d}{dr}\left(r\frac{dT}{dr}\right)+\mu\left(\frac{du}{dr}\right)^2=\rho c_p u\frac{dT_b}{dz} \tag{7}$$

The thermal boundary conditions are:

$$\text{Case A}: \begin{cases} -k\dfrac{\partial T}{\partial r} = q_i & \text{at } r = R_i \\ k\dfrac{\partial T}{\partial r} = 0 & \text{at } r = R_o \end{cases} \tag{8}$$

$$\text{Case B}: \begin{cases} -k\dfrac{\partial T}{\partial r} = 0 & \text{at } r = R_i \\ k\dfrac{\partial T}{\partial r} = q_o & \text{at } r = R_o \end{cases} \tag{9}$$

where the wall heat fluxes, q_i and q_o, are taken as positive into the fluid.

T_b is the bulk temperature defined as

$$T_b \equiv \int_{R_i}^{R_o} uT\cdot 2\pi r dr \Big/ \int_{R_i}^{R_o} u\cdot 2\pi r dr \tag{10}$$

By integrating Eq.(7) with Eq.(8) or Eq.(9), dT_b/dz is obtained as:

$$\frac{dT_b}{dz}=\frac{2R_j q_j}{\rho c_p u_m(R_o^2-R_i^2)}\left[1+\frac{\int_{R_i}^{R_o}\mu r\left(\frac{du}{dr}\right)^2 dr}{R_j q_j}\right] \tag{11}$$

where j = i for Case A and j = o for Case B.

Dimensionless temperature, θ, is defined as

$$\theta \equiv T/[q_j(R_o-R_i)/k] \tag{12}$$

Equation (11) may be expressed in dimensionless form as

$$\frac{d\theta_b}{d\eta}=\frac{8R_j}{R_o(1+\alpha)}\left(1+\frac{R_o}{R_j}Br_j\cdot V_B\right) \tag{13}$$

where

$$\eta \equiv \frac{z}{2(R_o-R_i)Pe} \tag{14}$$

$$Br_j \equiv \frac{\mu u_m^2}{(1-\alpha)R_o q_j} \quad \text{(Brinkman number)} \tag{15}$$

$$V_B \equiv (1-\alpha)\left[\int_\alpha^1 r^*\left(\frac{du^*}{dr^*}\right)^2 dr^*\right]$$

$$= 4(1-\alpha)(1-\alpha^2)\left[\frac{(1-EU^*)}{M}\right]^2$$

$$\times(1+\alpha^2-2B^*+B^*w) \tag{16}$$

The energy equation and the boundary conditions may be expressed in dimensionless form as

$$\frac{1}{r^*}\frac{d}{dr^*}\left(r^*\frac{d\theta}{dr^*}\right) = \left[\frac{2S}{(1+\alpha)(1-\alpha)^2}\right]u^* + Br_j \cdot V \quad (17)$$

$$\text{Case A}: \begin{cases} \frac{d\theta}{dr^*} = \frac{1}{\alpha-1} & \text{at } r^* = \alpha \\ \frac{d\theta}{dr^*} = 0 & \text{at } r^* = 1 \end{cases} \quad (18)$$

$$\text{Case B}: \begin{cases} \frac{d\theta}{dr^*} = 0 & \text{at } r^* = \alpha \\ \frac{d\theta}{dr^*} = \frac{1}{1-\alpha} & \text{at } r^* = 1 \end{cases} \quad (19)$$

where $S = \alpha$ for Case A and $S = 1$ for Case B.

The parameter V is related to viscous dissipation, defined as

$$V \equiv \left[\frac{2}{(1+\alpha)(1-\alpha)^2}\cdot V_B\right]u^* - \left(\frac{du^*}{dr^*}\right)^2$$
$$= 8\left[\frac{(1-EU^*)}{M}\right]^2(1+\alpha^2-2B^*+B^*w)u^* - \left(\frac{du^*}{dr^*}\right)^2 \quad (20)$$

Nusselt numbers, Nu_{jj}, on the inner and outer walls are calculated as

$$Nu_{jj} \equiv \frac{[q_j/(T_j - T_b)]2(R_o - R_i)}{k} = \frac{2}{\theta_j - \theta_b} \quad (21)$$

The dimensionless bulk temperature, θ_b, is defined as

$$\theta_b \equiv T_b / [q_j(R_o - R_i)/k] \quad (22)$$

$(\theta_j - \theta_b)$ is calculated as

$$\theta_j - \theta_b = \left(\frac{2}{1-\alpha^2}\right)\int_\alpha^1 r^* u^*(\theta_j - \theta)dr^* \quad (23)$$

Case A: In this case, Eq.(13) with j= i is written as

$$\frac{d\theta_b}{d\eta} = \frac{8\alpha}{(1+\alpha)}\left(1 + \frac{1}{\alpha}Br_i \cdot V_B\right) \quad (24)$$

The temperature difference is obtained as

$$\theta_i - \theta = -\frac{(1-EU^*)}{M}\left[c_1 r^{*2} + c_2 r^{*4} + c_3 r^{*2}\ln r^* + c_4(\ln r^*)^2 + a_1 \ln r^* + a_2\right] \quad (25)$$

where θ_i is the dimensionless inner wall temperature and the coefficients c_1, c_2, c_3, c_4, a_1 and a_2 are

$$c_1 = \left[\frac{\alpha(1-B^*)}{(1+\alpha)(1-\alpha)^2}\right] + 4Br_i \times \left[\frac{(1+\alpha^2) + \{w-2+(w-1)(2\alpha^2-B^*)\}B^*}{\{1+(2w-1)\alpha^2 - B^*\}^2}\right] \quad (26)$$

$$c_2 = -\frac{1}{4}\left[\frac{\alpha}{(1+\alpha)(1-\alpha)^2}\right] - Br_i\left[\frac{2+2w\alpha^2+(w-3)B^*}{\{1+(2w-1)\alpha^2-B^*\}^2}\right] \quad (27)$$

$$c_3 = \left[\frac{\alpha B^*}{(1+\alpha)(1-\alpha)^2}\right] + 4Br_i\left[\frac{\{1+\alpha^2+(w-2)B^*\}B^*}{\{1+(2w-1)\alpha^2-B^*\}^2}\right] \quad (28)$$

$$c_4 = -2Br_i\left[\frac{B^{*2}}{1+(2w-1)\alpha^2-B^*}\right] \quad (29)$$

$$a_1 = -(2c_1 + 4c_2 + c_3) \quad (30)$$

$$a_2 = -[c_1\alpha^2 + c_2\alpha^4 + c_3\alpha^2\ln\alpha + c_4(\ln\alpha)^2 + a_1\ln\alpha] \quad (31)$$

Nusselt number is calculated as

$$Nu_{ii}^{(2)} = 2[1+(2w-1)\alpha^2 - B^*]^2/G_{ii} \quad (32)$$

where

$$G_{ii} = g_{i1} + g_{i2}\alpha^2 + g_{i3}\alpha^4 + g_{i4}\alpha^6 \quad (33)$$

$$g_{i1} = -\left(\frac{1}{3}-\frac{B^*}{4}\right)c_1 - \left(\frac{1}{6}-\frac{B^*}{9}\right)c_2 + \left(\frac{5}{36}-\frac{B^*}{8}\right)c_3 - \left(\frac{7}{8}-\frac{3B^*}{2}\right)c_4 + \left(\frac{3}{4}-B^*\right)a_1 - (1-B^*)a_2 \quad (34)$$

$$g_{i2} = -\left(\frac{1}{3}-\frac{B^*}{4}\right)c_1 - \left(\frac{1}{6}-\frac{B^*}{9}\right)c_2 + \left(\frac{5}{36}-\frac{B^*}{8}\right)c_3 + \left[\left(\frac{1}{8}-3w\right) + \frac{(2-3w)}{B} + \frac{2(1-w)}{B^2}\right]c_4 - \left[\left(\frac{1}{4}-2w\right) + \frac{2(1-w)}{B}\right]a_1 + (1-2w)a_2 \quad (35)$$

$$g_{i3} = \left(\frac{2}{3}-w\right)c_1 - \left(\frac{1}{6}-\frac{B^*}{9}\right)c_2 - \left[\left(\frac{1}{9}-\frac{w}{2}\right) + \frac{(1-w)}{B}\right]c_3 - \left[\frac{(1-6w)}{2B} + \frac{(3-4w)}{B^2}\right]c_4 + \left[\frac{(1-2w)}{B}\right]a_1 \quad (36)$$

$$g_{i4} = \left(\frac{1}{2} - \frac{2w}{3}\right)c_2 + \left[\frac{(2-3w)}{3B}\right]c_3 + \left[\frac{(1-2w)}{B^2}\right]c_4 \quad (37)$$

Case B: Equation (13) with $j = o$ is written as

$$\frac{d\theta_b}{d\eta} = \frac{8}{(1+\alpha)}(1 + Br_o \cdot V_B) \quad (38)$$

The temperature difference is obtained as

$$\theta_o - \theta = -\frac{(1-EU^*)}{M}\left[d_1 r^{*2} + d_2 r^{*4} + d_3 r^{*2}\ln r^* + d_4(\ln r^*)^2 + b_1 \ln r^* + b_2\right] \quad (39)$$

where θ_o is the dimensionless outer wall temperature and the coefficients d_1, d_2, d_3, d_4, b_1 and b_2 are

$$d_1 = \left[\frac{(1-B^*)}{(1+\alpha)(1-\alpha)^2}\right] + 4Br_o \times \left[\frac{(1+\alpha^2) + \{w - 2 + (w-1)(2\alpha^2 - B^*)\}B^*}{\{1 + (2w-1)\alpha^2 - B^*\}^2}\right] \quad (40)$$

$$d_2 = -\frac{1}{4}\left[\frac{1}{(1+\alpha)(1-\alpha)^2}\right] - Br_o\left[\frac{2 + 2w\alpha^2 + (w-3)B^*}{\{1 + (2w-1)\alpha^2 - B^*\}^2}\right] \quad (41)$$

$$d_3 = \left[\frac{B^*}{(1+\alpha)(1-\alpha)^2}\right] + 4Br_o\left[\frac{\{1 + \alpha^2 + (w-2)B^*\}B^*}{\{1 + (2w-1)\alpha^2 - B^*\}^2}\right] \quad (42)$$

$$d_4 = -2Br_o\left[\frac{B^{*2}}{1 + (2w-1)\alpha^2 - B^*}\right] \quad (43)$$

$$b_1 = -[(2d_1 + d_3)\alpha^2 + 4d_2\alpha^4 + 2d_3\alpha^2\ln\alpha + 2d_4\ln\alpha] \quad (44)$$

$$b_2 = -(d_1 + d_2) \quad (45)$$

Nusselt number is determined as

$$Nu_{oo}^{(2)} = 2[1 + (2w-1)\alpha^2 - B^*]^2 / G_{oo} \quad (46)$$

where

$$G_{oo} = g_{o1} + g_{o2}\alpha^2 + g_{o3}\alpha^4 + g_{o4}\alpha^6 \quad (47)$$

$$g_{o1} = -\left(\frac{1}{3} - \frac{B^*}{4}\right)d_1 - \left(\frac{1}{6} - \frac{B^*}{9}\right)d_2 + \left(\frac{5}{36} - \frac{B^*}{8}\right)d_3 - \left(\frac{7}{8} - \frac{3B^*}{2}\right)d_4 + \left(\frac{3}{4} - B^*\right)b_1 - (1-B^*)b_2 \quad (48)$$

$$g_{o2} = -\left(\frac{1}{3} - \frac{B^*}{4}\right)d_1 - \left(\frac{1}{6} - \frac{B^*}{9}\right)d_2 + \left(\frac{5}{36} - \frac{B^*}{8}\right)d_3 + \left[\left(\frac{1}{8} - 3w\right) + \frac{(2-3w)}{B} + \frac{2(1-w)}{B^2}\right]d_4 - \left[\left(\frac{1}{4} - 2w\right) + \frac{2(1-w)}{B}\right]b_1 + (1-2w)b_2 \quad (49)$$

$$g_{o3} = \left(\frac{2}{3} - w\right)d_1 - \left(\frac{1}{6} - \frac{B^*}{9}\right)d_2 - \left[\left(\frac{1}{9} - \frac{w}{2}\right) + \frac{(1-w)}{B}\right]d_3 - \left[\frac{(1-6w)}{2B} + \frac{(3-4w)}{B^2}\right]d_4 + \left[\frac{(1-2w)}{B}\right]b_1 \quad (50)$$

$$g_{o4} = \left(\frac{1}{2} - \frac{2w}{3}\right)d_2 + \left[\frac{(2-3w)}{3B}\right]d_3 + \left[\frac{(1-2w)}{B^2}\right]d_4 \quad (51)$$

3. Result and Discussion

3.1 Effects of moving core velocity

The effects of the relative velocity of the moving core U^* on the velocity profiles across the annulus for the cases of α = 0.2, 0.5 and 0.8 are shown in Fig.2. It is seen clearly that the profiles of the fluid velocity are deformed by the moving core with a relative velocity U^*. For $U^* < 0$, the velocity profile is parabolic having a larger maximum value with increasing values of α.

The velocity gradient and parameter V govern the heat transfer with viscous dissipation through Eq.(16). The behaviors of velocity gradient and V are shown in terms of $(1-\alpha)^2(du^*/dr^*)^2$ and $(1-\alpha)^2 V$, respectively, in Figs.3 and 4, for α = 0.2, 0.5 and 0.8. The absolute values of velocity gradient and V become larger near the moving wall ($\zeta = 0$) with a decrease in U^*.

Figure 5 shows the magnitude of parameter V_B. It is seen that V_B increases with a decrease in U^*.

In Fig.6, the magnitude of $d\theta_b/d\eta$ is shown for Cases A and B respectively. It is seen from these figures that $d\theta_b/d\eta$ changes sharply with α for $U^* = -2$, and depends weakly

on α for $U^* = 0$ and $U^* = 2$. $d\theta_b / d\eta$ increases with an increase in Br_j.

In Figs.7 and 8, the effect of U^* on the dimensionless temperature differences $(\theta_i - \theta)$, $(\theta_o - \theta)$ and $(\theta - \theta_b)$, are shown respectively for Cases A and B. $(\theta_i - \theta)$ decreases with an increase in U^* near the fixed wall, but $(\theta_o - \theta)$ increases with an increase in U^* near the moving wall. $(\theta - \theta_b)$ decreases with an increase in U^* near the moving wall for Cases A and B.

In Fig.9 Nusselt numbers, Nu_{jj}, for Cases A and B are shown. From these figures it is seen that Nu_{jj} changes clearly with an increase in U^* for Case A and depends weakly on U^* for Case B.

3.2 Effects of viscous dissipation

In both Cases of A and B, $d\theta_b / d\eta$ increases with an increase in Brinkman number, Br_j for heating process ($Br_j > 0$) and decreases with an increase in Br_j for cooling process ($Br_j < 0$) (see Fig.6).

In Case A, $(\theta_i - \theta)$ increases with an increase in Br_i for $U^* = -2$ and $U^* = 0$, whereas it decreases with an increase in Br_i for $U^* = 2$ (see Fig.7). In Case B, $(\theta_o - \theta)$ decreases with an increase in Br_o for $U^* = -2$, whereas it increases with an increase in Br_o for $U^* = 0$ and $U^* = 2$ (see Fig.7).

In Cases A and B, for $Br_j > 0$ and $U^* = 0$ the bulk temperature difference $(\theta - \theta_b)$ increases with an increase in Br_j near the walls (see Fig.8). But it decreases in the middle section. This is attributed to that near the walls the dimensionless velocity gradient is large (see Fig.3) and that the viscous dissipation effect is large. The heat axially transfered by convection is large in the middle section (see Fig.2). For $U^* = -2$, $(\theta - \theta_b)$ greatly increases with an increase in Br_j near the moving wall, but increases a little near the fixed wall. In the middle section it decreases. The dimensionless velocity gradient is large near the moving wall and small near the fixed wall. For $U^* = 2$, $(\theta - \theta_b)$ increases with an increase in Br_j near the fixed wall and decreases near the moving wall. Near the moving wall the dimensionless velocity gradient is large, but small near the fixed wall (see Fig.3). The heat transfered by convection is larger near the moving wall (see Fig.2).

Nusselt numbers, Nu_{jj} increases with an increase in Br_i for Case A and it decreases with an in Br_o for Case B (see Fig.9).

3.3 Cooling process

The negative values for Br_j correspond to the cooling process. In Figs.10 and 11, the effects of U^* and viscous dissipation on the dimensionless temperatures $(\theta_i - \theta)$, $(\theta_o - \theta)$ and $(\theta - \theta_b)$, are shown respectively for Cases A and B. In cooling processes the behavior of temperature differences tends to be contrary to that in heating process (see Figs.7 and 8).

The effects of viscous dissipation in cooling process are shown for Cases A and B in Fig.12. It is seen from these figures that Nusselt numbers depend on Br_j and U^*. Especially, the behaviors of Nu_{jj} vary widely when the value of Br_j is large.

4. Conclusions

The study showed that for equal conditions the following changes were observed in heating process.

a) With an increase in U^*,

- decrease in $d\theta_b / d\eta$ for Cases A and B
- decrease in $\theta_i - \theta$ for Case A
- increase in $\theta_o - \theta$ for Case B
- decrease in $\theta - \theta_b$ for Cases A and B
- increase in Nu_{ii} for Case A
- decrease in Nu_{oo} for Case B

b) With an increase of Br_j

- increase in $d\theta_b / d\eta$ for Cases A and B
- increase in $\theta_i - \theta$ $(U^* \leq 0)$ and decrease in $\theta_i - \theta$ $(U^* > 0)$ for Case A
- decrease in $\theta_o - \theta$ $(U^* < 0)$ and increase in $\theta_o - \theta$ $(U^* \geq 0)$ for Case B
- decrease in $\theta - \theta_b$ for Cases A and B
- decrease in Nu_{ii} $(U^* < 0.4)$ and increase in Nu_{ii} $(U^* \geq 0.4)$ for Case A
- decrease in Nu_{oo} for Case B

The effect of Br_j on $d\theta_b / d\eta$, $\theta_j - \theta$, and $\theta - \theta_b$ is stronger for $U^* < 0$. But it affects more strongly on Nu_{ii} (Case A) when $U^* > 0$.

References

1. C. P. Tso and S. P. Manulikar "The use of the Brinkman number for single phase forced convective heat transfer in microchannels"
*Int.J.Heat Mass Transfer, vol.*41, No.12, p.1759-1769 (1998).

2. T. Shigechi and Y. Lee "An analysis on fully developed laminar fluid flow and heat transfer in concentric annuli with moving cores"
*Int.J.Heat Mass Transfer, vol.*34, No.10, p.2593-2601 (1991).

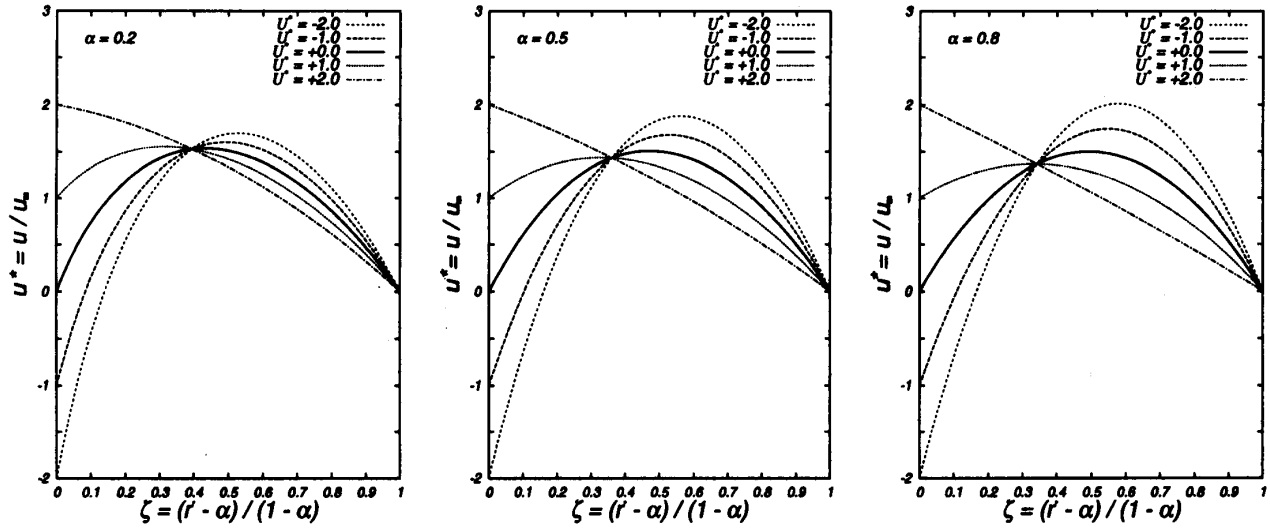

Fig.2 Velocity profiles

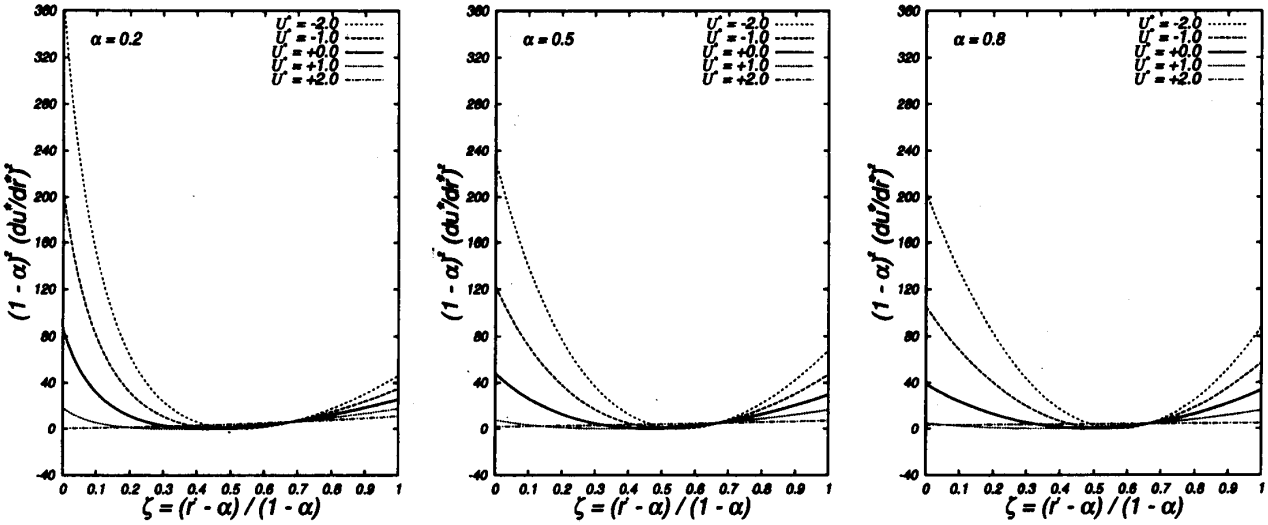

Fig.3 Square of velocity gradient

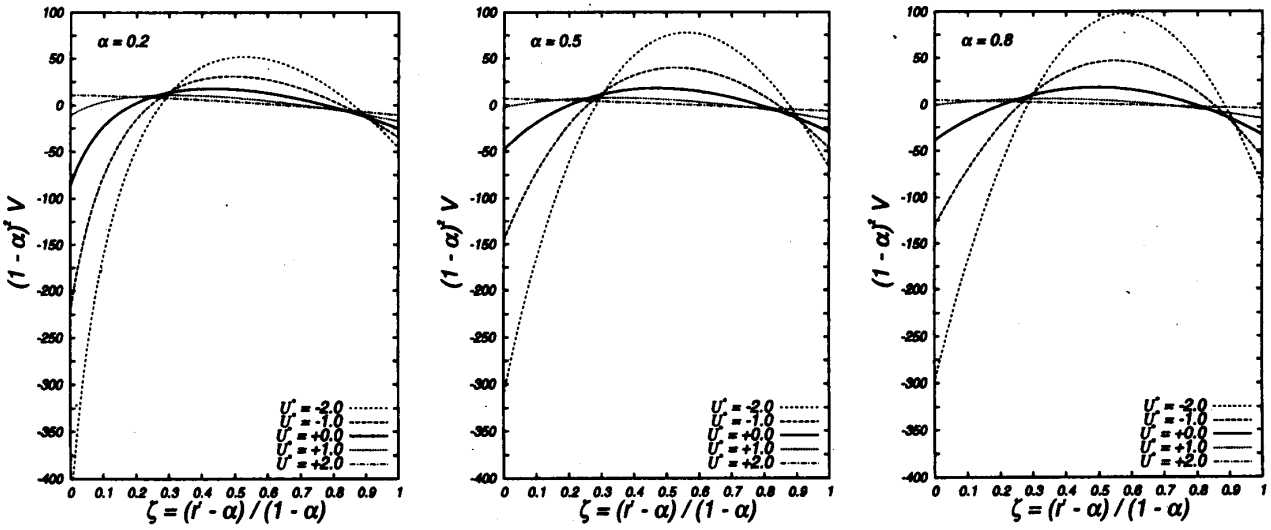

Fig.4 Distribution of parameter V

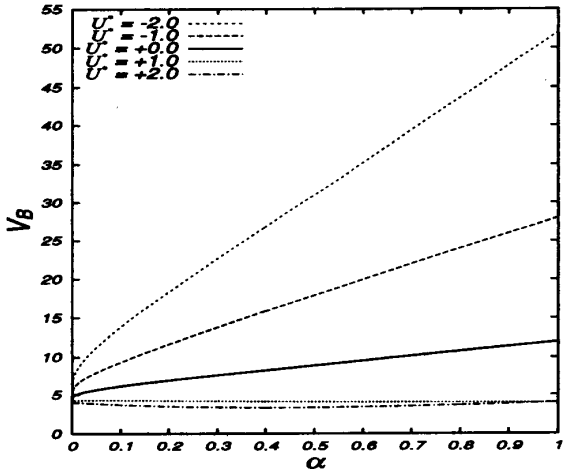

Fig.5 Magnitude of parameter V_B

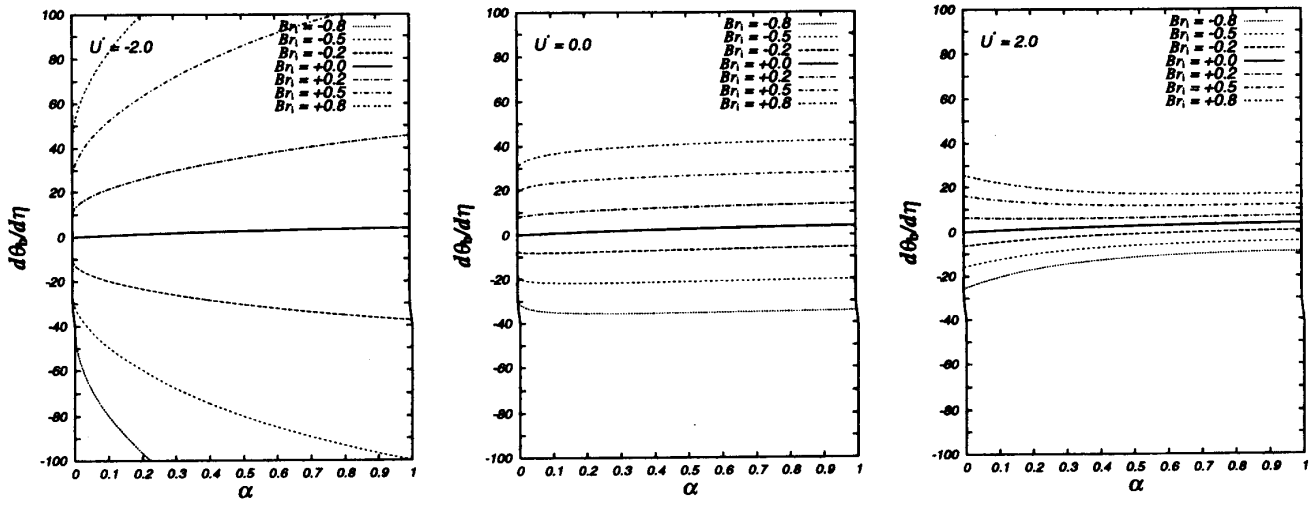

Case A

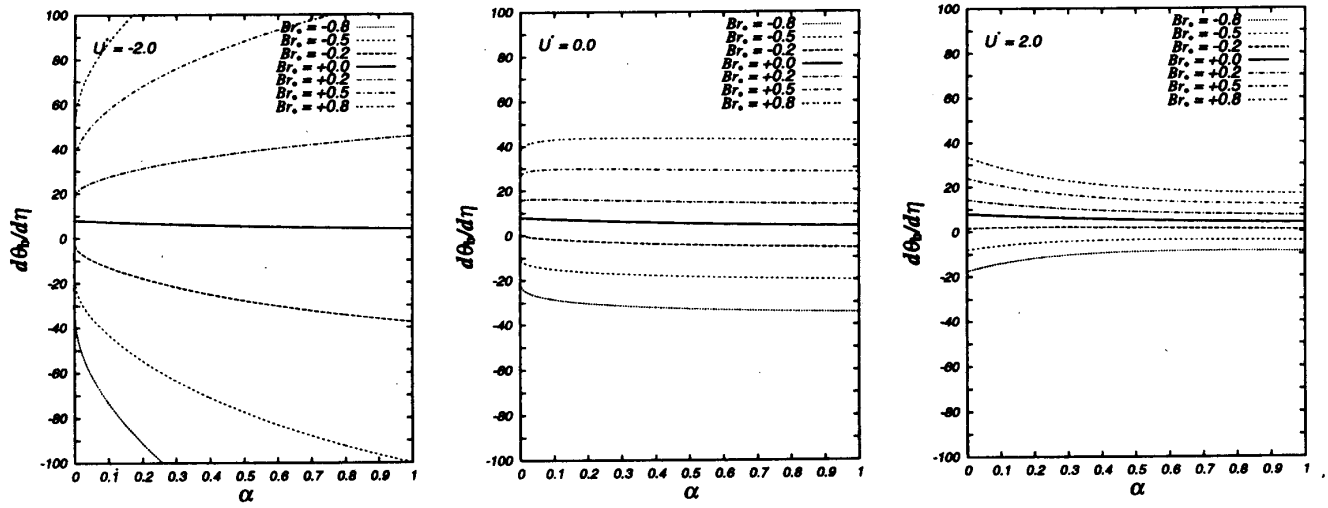

Case B

Fig.6 $\dfrac{d\theta_b}{d\eta}$ vs. α

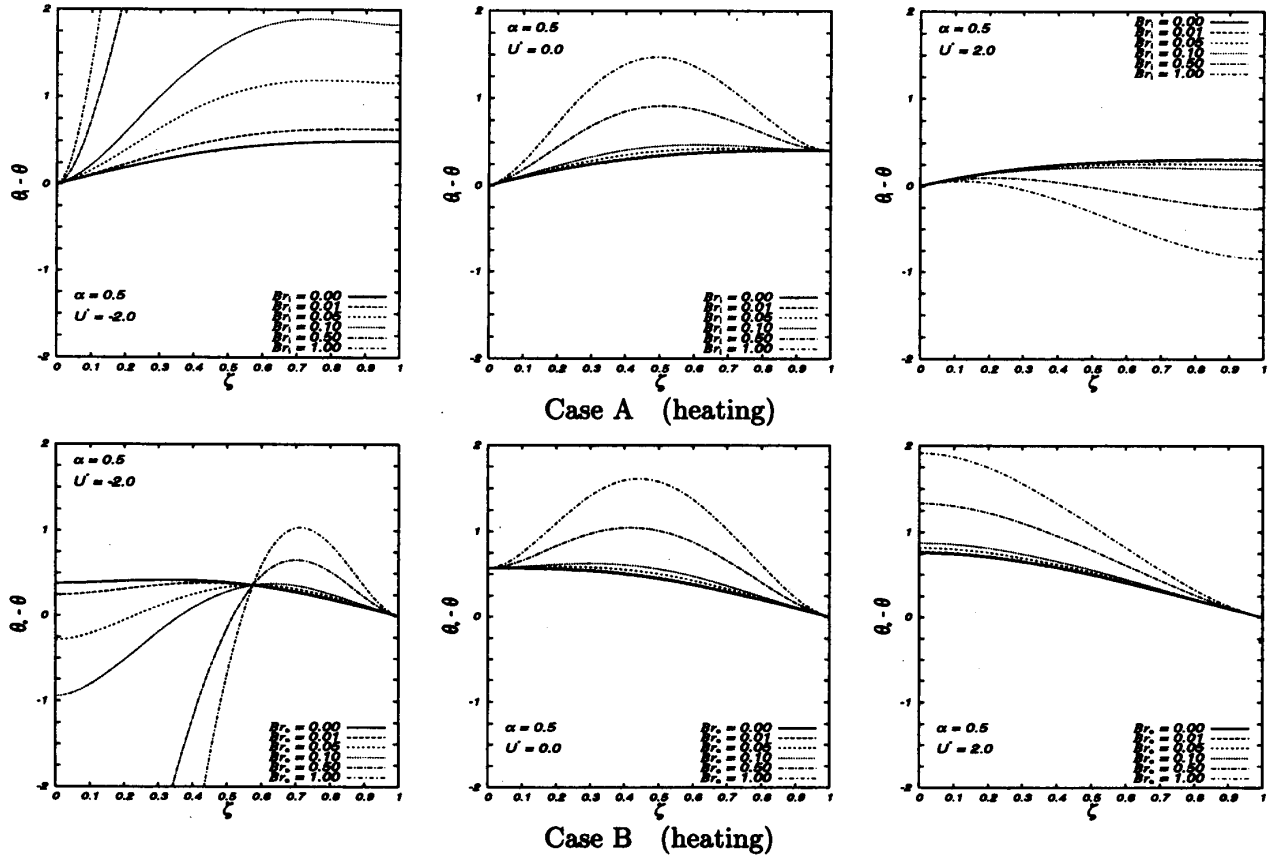

Fig.7 Dimensionless temperature difference ($\theta_J - \theta$) for Cases A and B

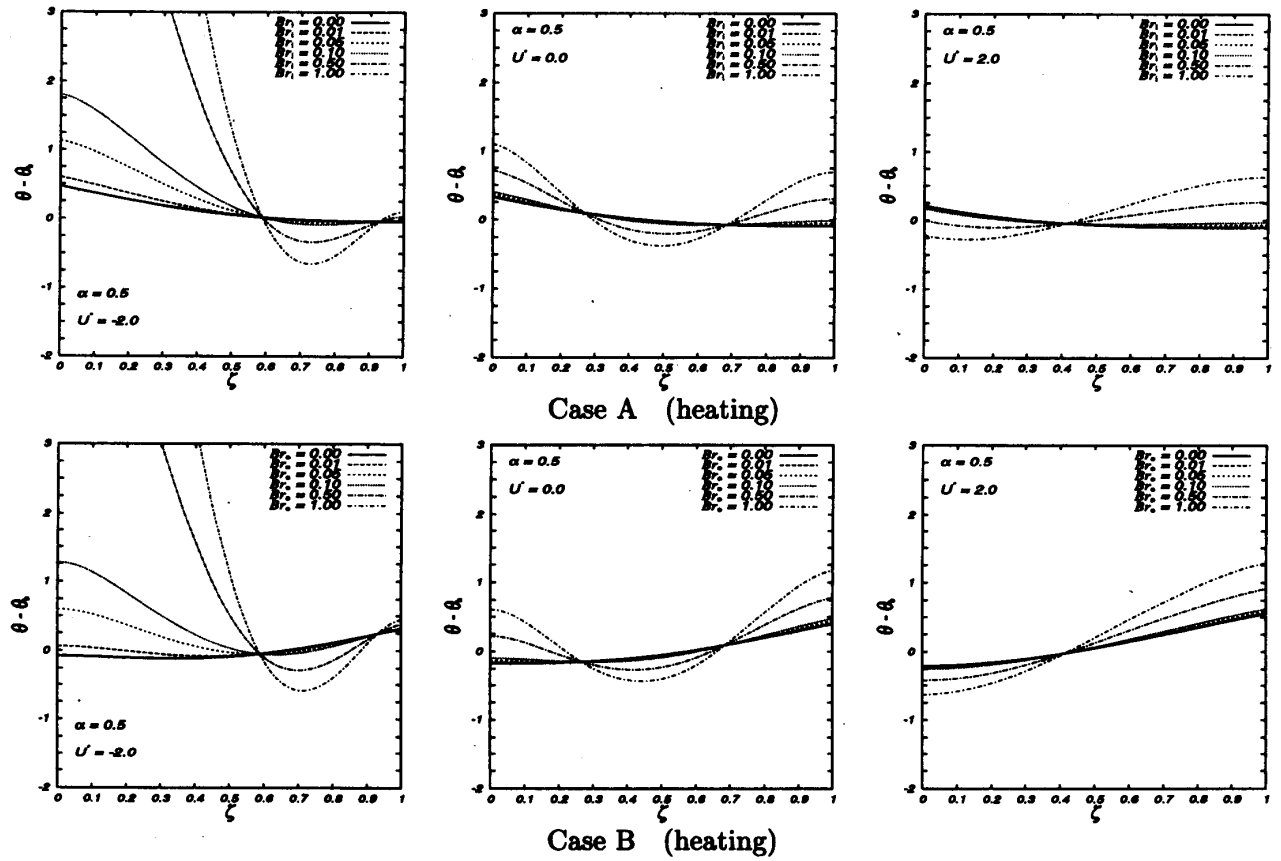

Fig.8 Dimensionless temperature difference ($\theta - \theta_b$) for Cases A and B

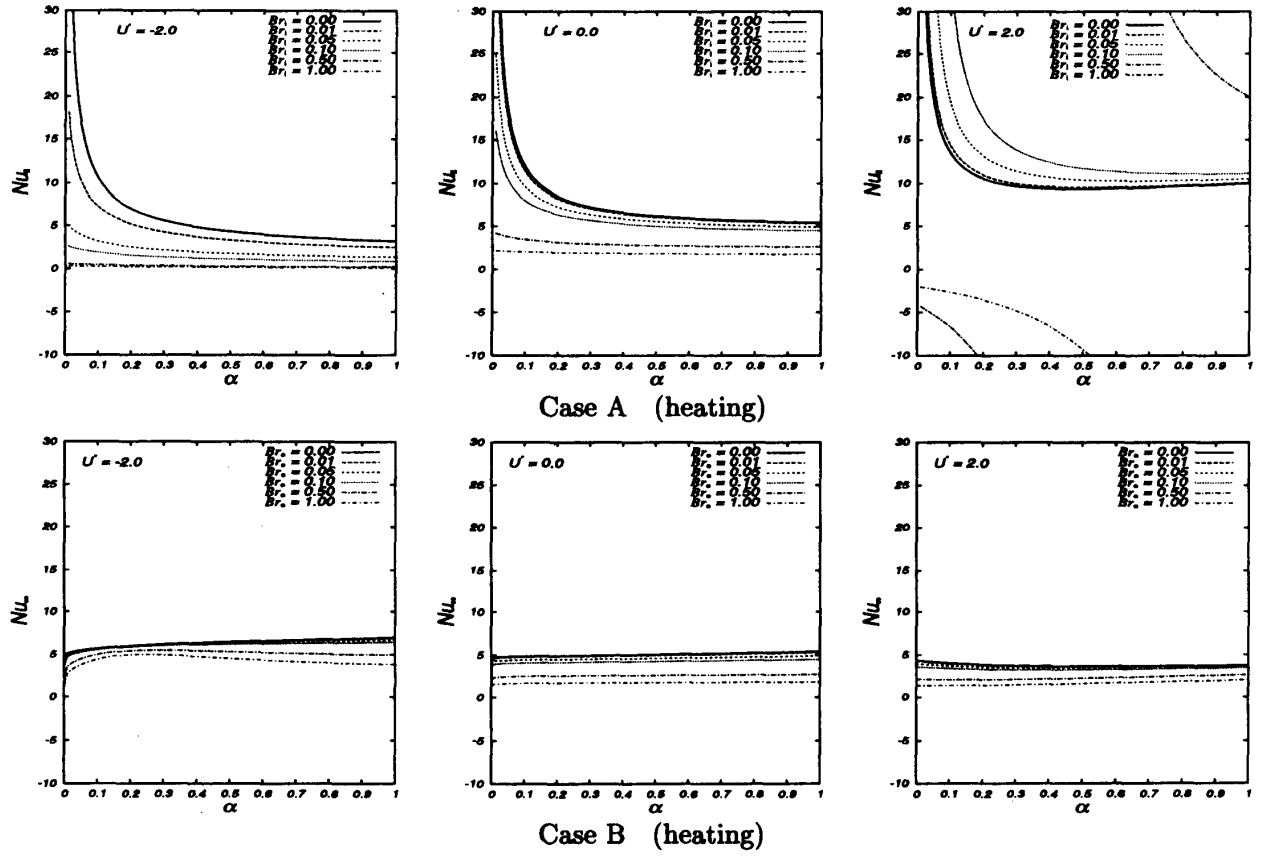

Fig.9 Nusselt numbers for Cases A and B

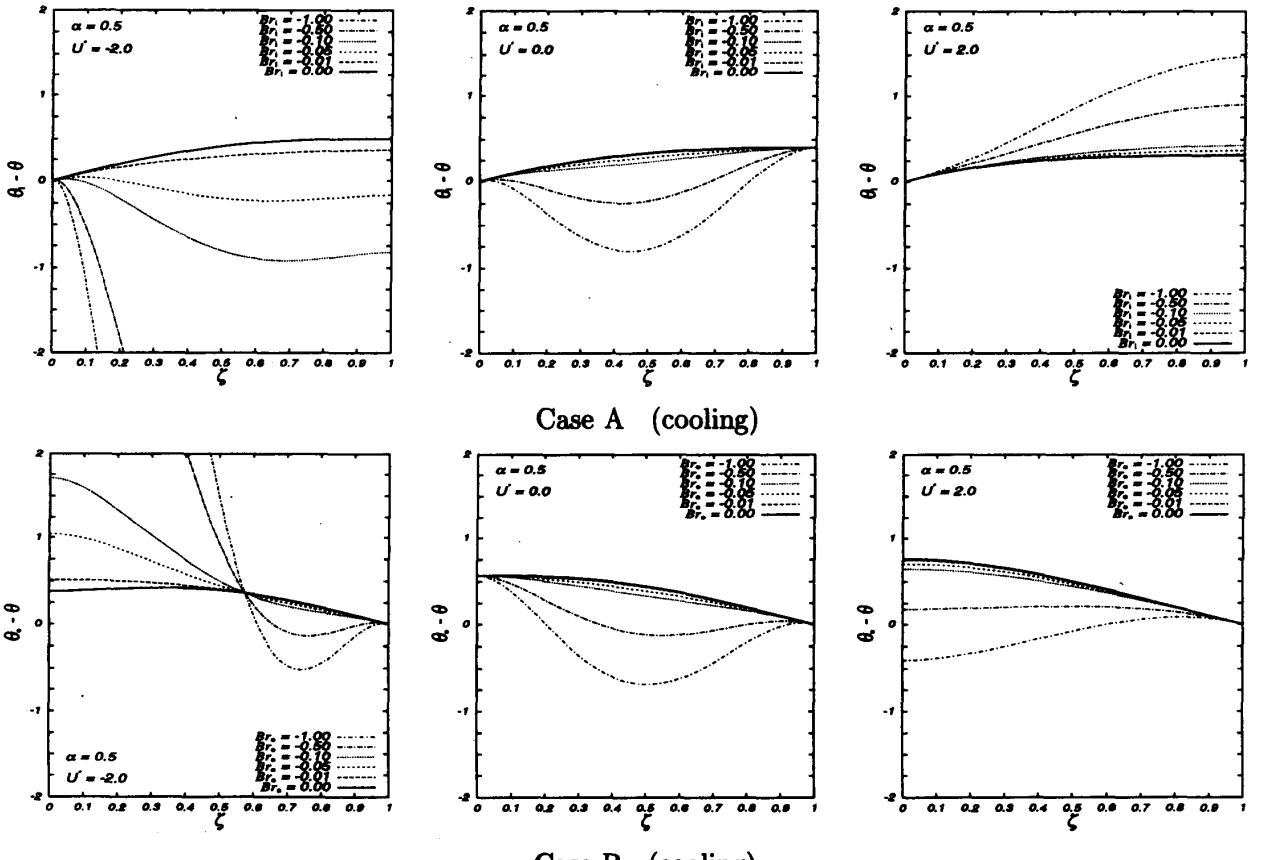

Fig.10 Dimensionless temperature difference ($\theta_1 - \theta$) for Cases A and B for cooling process

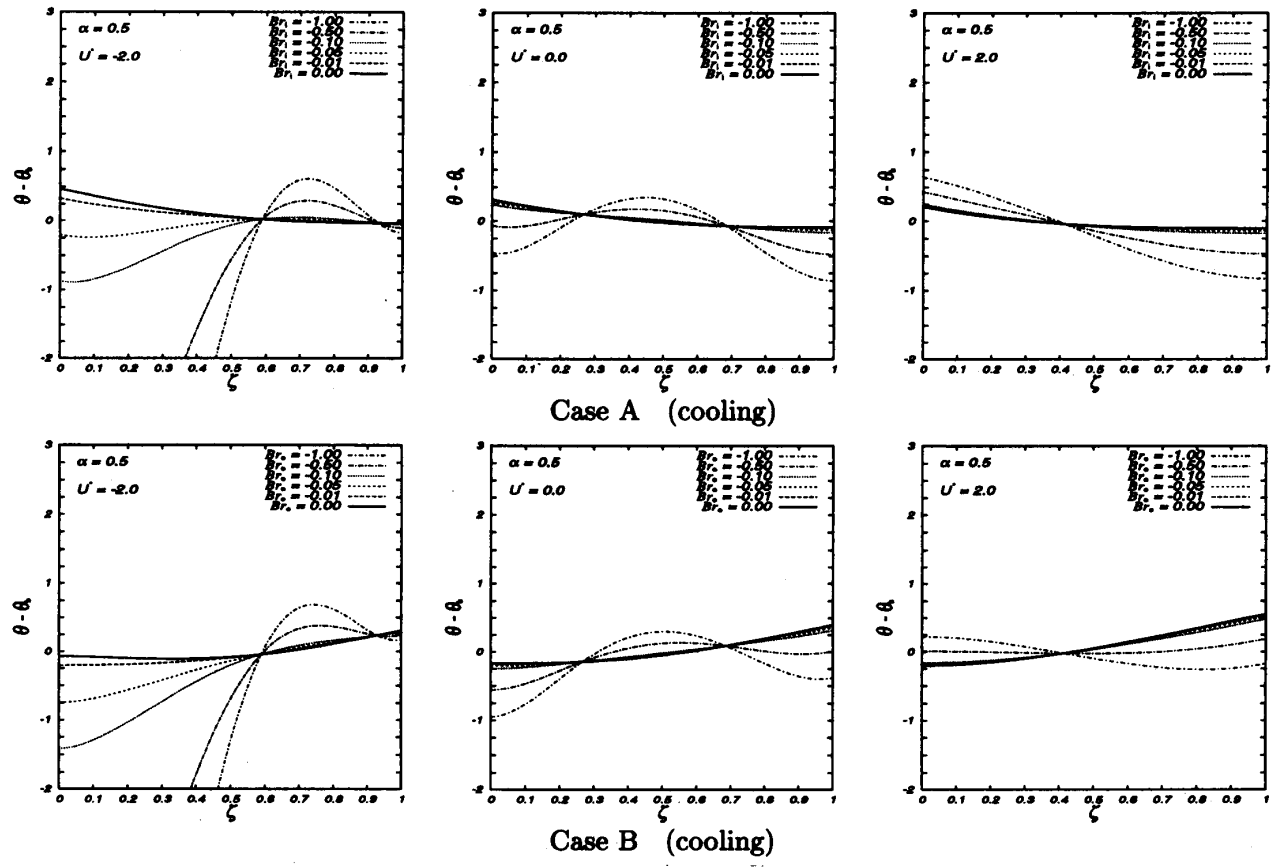

Fig.11 Dimensionless temperature difference ($\theta - \theta_b$) for Cases A and B for cooling process

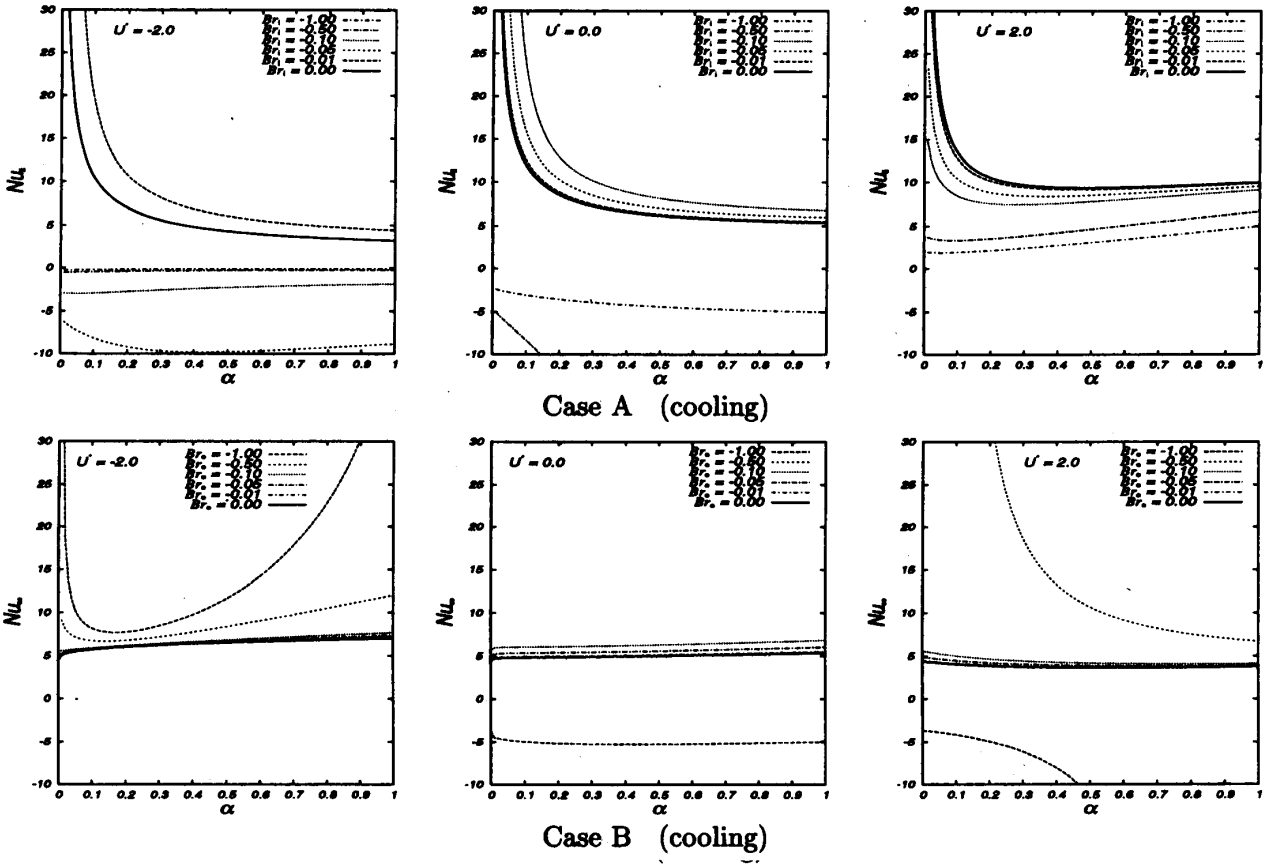

Fig.12 Nusselt numbers for Cases A and B for cooling process